



## CALCULATION OF VISCOUS ENERGY DISSIPATION IN ASPHALT PAVEMENTS

Simon Pouget<sup>1</sup>✉, Cédric Sauzéat<sup>2</sup>, Hervé Di Benedetto<sup>3</sup>, François Olard<sup>4</sup>

<sup>1,4</sup>EIFFAGE Travaux Publics, 8 rue du dauphiné 69960 Corbas, France

<sup>2,3</sup>Dept of Civil Engineering and Building, University of Lyon, ENTPE (FRE CNRS 3237),  
3 rue Maurice Audin 69518 Vaulx-en-Velin, France

E-mails: <sup>1</sup>simon.pouget@eiffage.com; <sup>2</sup>cedric.sauzeat@entpe.fr; <sup>3</sup>herve.dibenedetto@entpe.fr;  
<sup>4</sup>francois.olard@eiffage.com

**Abstract.** This paper presents a method to evaluate the energy dissipation in the pavement, induced by the viscous behaviour of bituminous constituents. The introduced method starts from the experimental characterization of each material and goes to the determination of stress and strain field, as well as viscous dissipated energy, in a pavement structure under a rolling wheel. A classical French pavement structure is considered as an application example. First, the behaviour of bituminous materials is characterized with advanced complex modulus tests. Second, a rheological model is used to describe the linear visco-elastic behaviour of bituminous materials. This model was previously developed at the Civil Engineering and Buildings Department of University of Lyon/ENTPE and has already shown its ability to describe completely and precisely the observed behaviour of bituminous materials. In order to make calculation the Finite Element software is then used in a third step, with the previous material model. Detailed hypotheses to perform the simulation of a rolling wheel on the pavement structure are explained. Results of the simulation are presented in terms of dissipated energy inside the pavement for a 40 ton truck. To give an order of magnitude, an estimation of the fuel consumption excess is given. Different temperature and vehicle speeds are considered. The Time Temperature Superposition Principle has been applied to estimate the dissipated energy at any temperature and vehicle speed. The simulation results show that energy dissipation in bituminous pavement due to the rolling weight of the considered 40 ton truck may induce a fuel consumption excess of a few percent for very unfavourable climatic conditions.

**Keywords:** pavement, energy dissipation, viscous behaviour, viscoelasticity, fuel consumption, Finite Element Model (FEM).

### 1. Introduction

Environmental aspects as well as sustainable development issue have become an important part of the decision-making processes for highway projects in many countries. Advantages of different road pavements (asphalt or concrete) from environmental and energy consumption points of view are therefore an important part of the planning processes.

The total energy consumption during construction and maintenance of roads is lower for asphalt pavements than that for concrete pavements (also greenhouse gas emissions). However, energy consumption of the vehicles is of huge importance (95 to 98%) during the lifetime of the road. Depending on the traffic volume the energy use for construction, maintenance and operation of the road is less than 2% to 5% of the energy used by the traffic itself (Beuving *et al.* 2004).

The transportation field represents currently 50% of global consumption of petroleum products and 21% of CO<sub>2</sub> emissions. In a world where petroleum becomes more and more rare and expensive and where policies to reduce greenhouse gases emissions tend to be put in place in many countries, the reduction of vehicle fuel consumption is of primary importance.

Many factors impact the fuel consumption of a vehicle. Among them, the main factors are the thermodynamic efficiency of the engine (to transfer heat into mechanical power), air resistance (effect of speed and aerodynamic shape) and rolling resistance (Fig. 1).

The quantification of energy dissipation of a pavement structure under wheel loading due to rolling resistance is then worthy of interest.

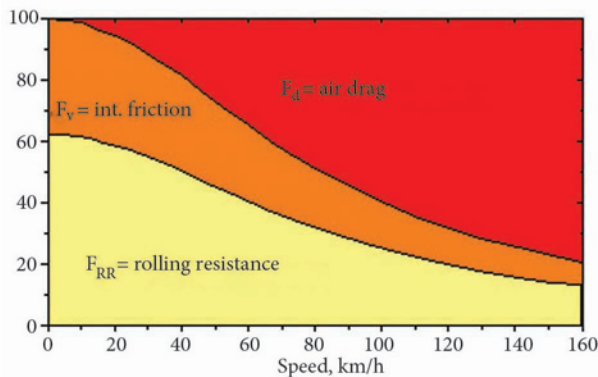
Approx 10% of fuel consumption for heavy trucks accounts for rolling resistance losses in the tires at a constant

speed of 80 km/h. This energy loss represents approximately 30% of the available power from the engine.

Passenger cars are normally overpowered and therefore have less efficient running engines, in particular gasoline fuelled engines. It is estimated that rolling resistance losses account for 15% to 20% of the fossil fuel input for such vehicles. At high speeds air drag becomes the largely predominant factor (Fig. 1). From a pavement point of view, two factors are influencing the rolling resistance:

- Evenness and texture (also referred as “pavement roughness” and mega-texture levels) of road surfaces (Fig. 1) have been proven to have a huge influence on vehicle fuel consumption (possible increase of 10% (Christophe et al. 1993). Taking these aspects into consideration might easily result in an advantage in fuel consumption for asphalt pavements (Beuving et al. 2004).

- The structural behaviour of pavements is reported to have a least influence on vehicle fuel consumption compared to evenness and roughness. Different studies tried to quantify the fuel consumption excess due to structural behaviour in bituminous pavements (Chupin et al. 2010; Du Plessis et al. 1990; Goos 2002; Ihs, Magnusson 2000; Laganier, Lucas 1990; Sandberg 1990; Williams 1981; Zaniewski et al. 1979; Zaniewski 1983). Even if it is difficult to identify the share due to the energy dissipated in the bituminous layers, a 1% excess in fuel consumption is generally reported in the previous references.



Force distribution in a passenger car with speed as percentage of the available power output at the crankshaft

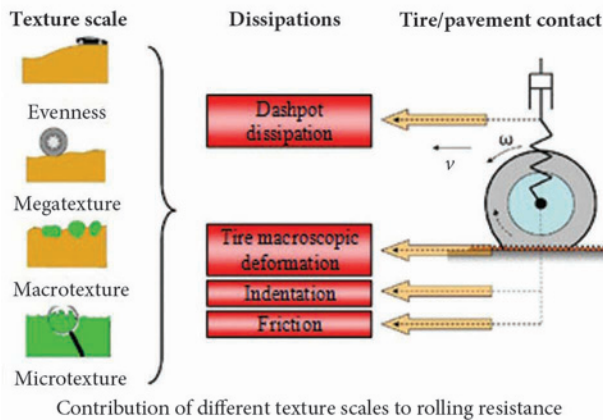


Fig. 1. Factors impact the fuel consumption of a vehicle

The constitutive materials of bituminous pavement structures have well-known linear viscoelastic behaviour for the small level of deformation existing in pavement structures. Therefore, linear viscoelasticity theory-related concepts may be used to estimate the viscous energy dissipation in bituminous pavements. An adapted modelling and finite element (FE) calculations are used and applied to a classical French pavement structure. Beyond the modelling considerations, the objective is to better understand the influence of both vehicle speed and pavement temperature.

In this paper a powerful method is proposed to calculate the dissipated viscous energy in pavements due to the viscoelastic behaviour of bituminous materials and then to evaluate resulting fuel consumption excess. Linear behaviour of each bituminous material is first determined experimentally and simulated using previous developed model in University of Lyon, which has already proved its efficiency. This model is implemented in Comsol FE software. Then simulations of a classical French pavement structure are performed to estimate the fuel excess consumption of a 40 t (ton) truck due to viscous dissipation. An original method based on the Time-Temperature Superposition Principle (TTSP) is proposed to determine viscous energy dissipation at any temperature and speed.

## 2. Pavement structure and materials behaviour

A traditional French pavement structure is chosen as reference. The subbase is represented by a 1.00 m thick soil foundation layer. A 0.06 m thick polymer modified asphalt (PMA) layer and a 2x0.08 m thick asphalt concrete (AC) layer constitute respectively the wearing course and the base course.

In this paper, only the linear behaviour is considered (small strain domain). No non-linearity (fatigue, permanent deformations, and cracks) is taken into account. The material constituting the subbase is considered as isotropic linear elastic. In the following, we focus on the behaviour of the bituminous materials (PMA and AC).

Complex modulus tests in tension/compression mode have been performed to characterize its linear viscoelastic behavior in the small strain domain ( $\epsilon < 10^{-4}$ ) (Baaj et al. 2005; Delaporte et al. 2009; Di Benedetto et al. 2004, 2011; Lundström et al. 2004)

Test equipment is used to apply sinusoidal cyclic loading (in tension and compression – trough zero) on cylindrical specimen of bituminous mix at different frequencies and temperatures. The size of samples is 80 mm diameter and 200 mm high. This tension-compression (push-pull) test creates homogeneous stress and strain fields in the middle of the tested specimen. A hydraulic press is associated with a temperature-controlled chamber (-60 °C to 80 °C) to monitor both loading and sample temperature. The load cell has a capacity of 10 kN. This system makes it possible to control either in stress or in strain mode. Axial strain is measured in the middle part of the specimen using three extensometers placed at 120°. During complex modulus tests, monitoring is made from the average of

three strain measurements. Measured sinusoidal signals are expressed in a complex form (Eq (1)).

$$\begin{cases} \sigma_z(t) = \sigma_{0z} \sin(\omega t) \\ \varepsilon_z(t) = \varepsilon_{0z} \sin(\omega t + \phi_{\varepsilon_z}) \end{cases} \quad (1)$$

where  $\sigma_{0z}$  and  $\varepsilon_{0z}$  – the amplitude of respectively axial stress and axial strain, while  $\phi_{\varepsilon_z}$  – the phase lag of axial strain in relation to axial stress.

Complex Young’s modulus  $E^*$  is then obtained using Eq (2). They are defined with its norm and phase angle, respectively  $|E^*|$  and  $\phi_E$  for  $E^*$ . Viscous energy dissipation is then calculated using Eq (3) and measurements from complex modulus tests for one cycle.

$$E^* = \frac{\sigma_z^*}{\varepsilon_z^*} = |E^*| e^{j\phi_E} = \frac{\sigma_{0z}}{\varepsilon_{0z}} e^{j\phi_{\varepsilon_z}} \quad (2)$$

$$W = \pi \sin(\phi_E) \sigma_{0z} \varepsilon_{0z} \quad (3)$$

Measurements were made at 9 different temperatures (from  $-30^\circ\text{C}$  to  $50^\circ\text{C}$ ), sweeping 7 frequencies from 0.01 Hz to 10 Hz. From experimental data, the TTSP is considered valid at a first approximation (some discrepancies appear at very low frequencies and for high temperatures, for PMA).  $E^*$  master curves (norm and phase angle) are plotted at a reference temperature ( $T_{ref}$ ) of  $10^\circ\text{C}$  in Fig. 2.

The first considered material (corresponding to the so-called “*Béton Bitumineux Semi-Grenu*” French specification) is bituminous mix made with a continuous 0/10 mm aggregate grading curve and 5.5% by weight of the aggregates of PMB (Polymer Modified Bitumen).

The second considered bituminous material (corresponding to the so-called “*Grave Bitume*” French specification) is AC made with a continuous 0/14 mm aggregate grading curve and 3.9% by weight of the aggregates of 35/50 penetration grade pure bitumen.

Shift factors considered for master curves construction are plotted in Fig. 3. The classical WLF (William, Landel and Ferry) law (Ferry 1980) is used to fit the shift factor  $a_T$  (Eq (4)).

$$\log(a_T) = -\frac{C_1(T - T_{ref})}{C_2 + T - T_{ref}} \quad (4)$$

with  $C_1 = 35$  and  $C_2 = 218$  for the PMA, and  $C_1 = 34$  and  $C_2 = 203$  for the AC.

Fig. 4 represents the energy dissipation obtained during one cycle of complex modulus test. Both possible control modes are used: set axial stress ( $\sigma_z$ , MPa) with an amplitude of 0.025 MPa and set axial strain ( $\varepsilon_z$ ,  $10^{-6}$ ) with an amplitude of  $40 \cdot 10^{-6}$ . This is compared with the results obtained from the DBN model (Di Benedetto *et al.* 2007, 2009; Neifar, Di Benedetto 2001; Mangiafico *et al.* 2013; Nguyen *et al.* 2009, 2012; Olard, Di Benedetto 2005; Pouget, Loup 2013; Tiouajni *et al.* 2011).

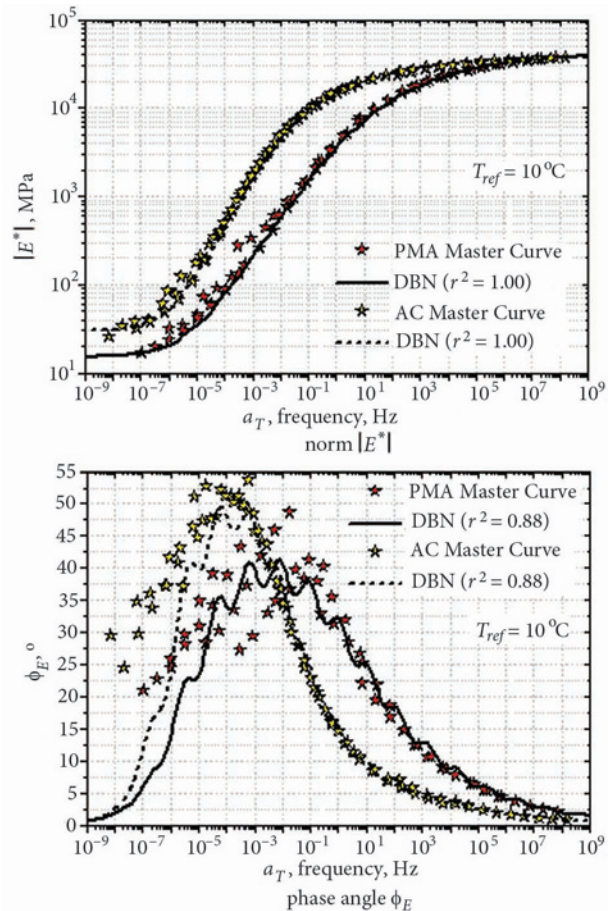


Fig. 2. Experimental master curves and DBN model simulation (20 elements) for complex Young’s modulus  $E^*$  of the two bituminous materials (PMA and AC) plotted at a reference temperature  $T_{ref} = 10^\circ\text{C}$

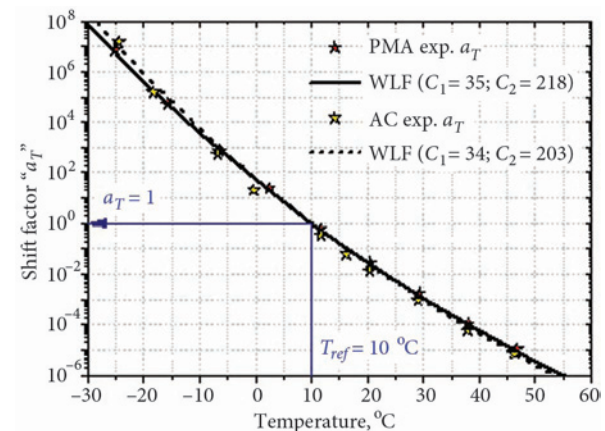


Fig. 3. Experimental and calculated shift factors (using WLF law) considered for construction of  $E^*$  and  $v^*$  master curves for the two bituminous materials (PMA and AC) plotted at  $T_{ref} = 10^\circ\text{C}$

The maximum energy dissipation does not appear at the same time for the different set modes and for the two materials. For the pavement structure, it is supposed that the solicitation is a combination of these two set modes.



Another interesting conclusion is that the maximum dissipation energy does not occur for the maximum value of the phase angle.

### 3. Viscous energy dissipation in asphalt pavement

Finite Element (FE) calculations are performed using COMSOL software considering 3D analysis. The linear visco-elastic model DBN has been implemented in the FE software as described in Pouget et al. (2010a, 2012a). This enables to simulate the behaviour of any pavement structures under any rolling load. These developments previously validated for orthotropic steel bridge and mix surfacing structures (Pouget et al. 2010a, 2010b, 2012c), are applied in

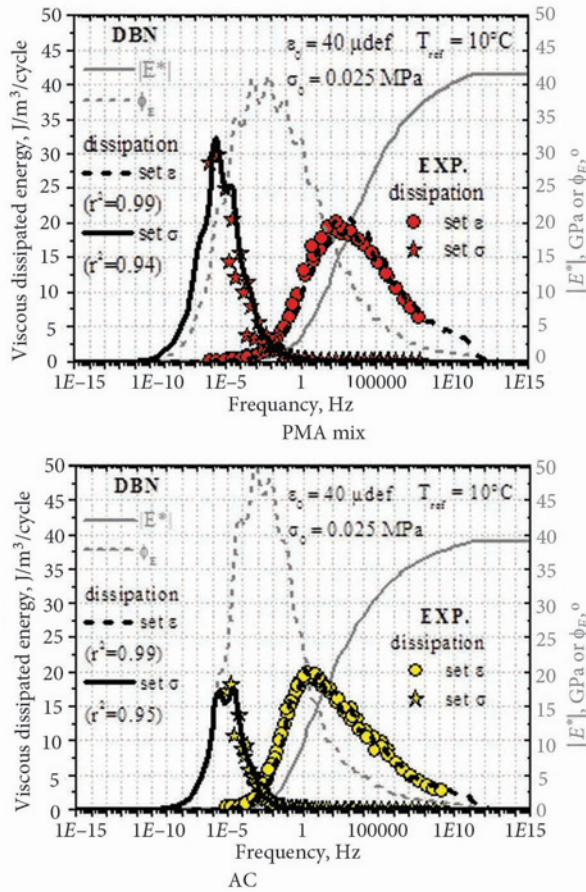


Fig. 4. Master curves of complex modulus norm  $|E^*|$  and phase angle  $\phi_E$  and viscous dissipated energy for set  $\sigma$  and set  $\epsilon$

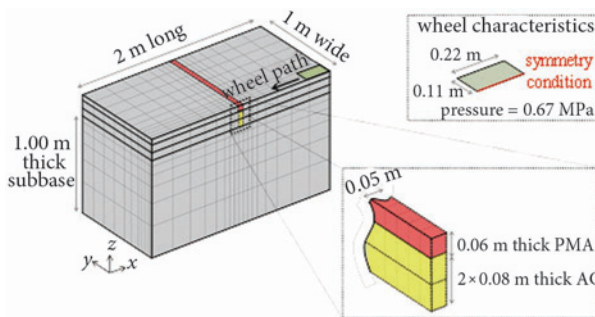


Fig. 5. 3D FE specimen geometry (mirror symmetry in the  $(x, z)$  plan) and a mesh used in the pavement response analysis

this paper on a classical French pavement structure. Stress and strain are evaluated in the pavement structure under a rolling wheel. Energy dissipation is calculated. Temperature and vehicle speed are also considered.

#### 3.1. Pavement structure

The pavement structure is represented by a 2 m long and 1 m wide slab (Fig. 5). The thickness of the different layers is the same as in the pavement previously presented in section called “Pavement structure”. A 1.00 m thick soil foundation layer constitutes the subbase. A 0.06 m thick PAM mix layer and a  $2 \times 0.08$  m thick AC layer constitute respectively the wearing course and the base course.

The FE mesh consists of 1360 Lagrange brick elements with a 2<sup>nd</sup> order interpolation function. The mesh is refined under the wheel path and in the centre of the slab (where dissipated energy is calculated).

The subbase material is isotropic linear elastic with a Young modulus  $E$  equal to 120 MPa and a Poisson’s ratio  $\nu$  equal to 0.35.

#### 3.2. Boundary conditions

The bottom side is clamped. The symmetry condition in the transversal way imposed boundary condition on one side. To ensure the continuity of this slab with the rest of pavement, only vertical displacement is allowed for other lateral sides.

A wheel, rolling at a constant speed in the longitudinal direction ( $x$  axis), is simulated. According to the French standard, the wheel load on the pavement is represented by a normal pressure of 0.67 MPa applied on a square area ( $0.22 \times 0.22$  m<sup>2</sup>).

Moreover, perfect bond is assumed between the different layers (Raab et al. 2013).

#### 3.3. Viscous energy dissipation

Once the stress-strain state has been obtained, the dissipated energy  $w(t)$  defined by Eq (5) is calculated for a volume  $V$  and a period  $t$ .

$$w(t) = \sum_{i=1}^n \iiint \left( \int \underline{\underline{\sigma}}_i : \underline{\underline{\dot{\epsilon}}}_i dt \right) dV, \quad (5)$$

where  $\underline{\underline{\sigma}}_i$  and  $\underline{\underline{\dot{\epsilon}}}_i$  – respectively the stress and strain rate in the body  $i$  of the DBN model.

Considering the previous development, Eq (5) is developed as shown in Eq (6).

$$w(t) = \sum_{i=1}^n \iiint \left( \int \frac{1}{\eta_i} \left( (1 + \nu_i) \cdot \left( \underline{\underline{\sigma}}_i^v : \underline{\underline{\sigma}}_i^v \right) - \nu_i \left( \text{tr} \left( \underline{\underline{\sigma}}_i^v \right) \right)^2 \right) dt \right) dV, \quad (6)$$

where  $k$  and  $l$  – the summation coefficients;  $\underline{\underline{\sigma}}_i^v$ ,  $\eta_i$  and  $\nu_i$  – respectively the viscous stress, the viscosity and the Poisson’s Ratio of the body  $i$  of the DBN model.

### 3.4. Results

The calculations are performed for different constant temperatures from  $-30\text{ }^{\circ}\text{C}$  to  $100\text{ }^{\circ}\text{C}$  and for 2 constant speeds (50 km/h and 100 km/h).

The dissipated energy per time  $w(t)$  is integrated on a 0.05 m long slice of the two bituminous materials, located in the centre of the 2 m long structure (Fig. 5). It is obtained at any time during the wheel passing. The dissipated energy is calculated separately in the wearing course constituted by the PMA and in the base course constituted by the AC. The obtained results are presented in Fig. 6 for 2 temperatures ( $10\text{ }^{\circ}\text{C}$  and  $63\text{ }^{\circ}\text{C}$ ) at 100 km/h for the half-wheel.

The total dissipated energy is equal to the sum of the energy dissipated by each bituminous layer. The results are plotted versus the time needed to cross the 2 m long structure at the considered speed. First, when the wheel is far from the considered central slice, its influence is negligible, especially at high temperatures. This validates the size of the chosen slab. Then as expected, for the lower temperature ( $10\text{ }^{\circ}\text{C}$ ) the dissipated energy is very weak compared to the one calculated at the intermediate temperature ( $63\text{ }^{\circ}\text{C}$ ) where the dissipation potential is huge.

From this result, the dissipated energy  $W_{truck}$  is calculated for a 40 t truck covering 1 km. First, the integration in time of last results gives the energy dissipated for a half wheel on this 0.05 m long slice. Then, the calculation is made for a 40 t truck (ten wheels as the one previously described are needed) and for 1 km (Eq (7)).

$$W_{truck} = \left( \int w(t).dt \right) \cdot 2 \cdot \frac{1\text{ km}}{0.05\text{ m}} \cdot 10. \quad (7)$$

This dissipated energy is compared to the total energy consumed to make the truck moving (without taking into account engine efficiency). The fuel consumption excess is evaluated using the proposed Eq (8):

$$\text{Fuel consumption excess} = \frac{W_{truck}}{(a).(b) / 100} \quad (8)$$

where  $a$  – fuel consumption of a 40 t truck is assumed to be 60 l/100 km;  $b$  – calorific value of the fuel is 40 MJ/l.

These parameters can be changed easily and therefore dissipated energy values and fuel consumption excess can be obtained for any type of vehicle (Fig. 7).

For a constant speed of 100 km/h, the dissipated energy presents a peak at  $63\text{ }^{\circ}\text{C}$ . The corresponding fuel consumption excess reaches approx. 5.5%. At low and very high temperatures, where bituminous material can be considered as purely elastic (in the small strain domain), energy dissipation is negligible. The critical temperature interval for which fuel consumption excess is consistent (more than 1%), ranges from  $40\text{ }^{\circ}\text{C}$  to  $90\text{ }^{\circ}\text{C}$ . This temperature level corresponds to the summer period in “in situ” condition (maximum road surface temperatures during summer period are reported to be in the range  $40\text{--}60\text{ }^{\circ}\text{C}$ ).

It is noteworthy, that at  $15\text{ }^{\circ}\text{C}$  – reference mean temperature for pavement design in France – for the same vehicle speed of 100 km/h, the increase in fuel consumption is equal to 0.25%.

The maximum dissipated energy in the different bituminous layers does not occur at the same time, as shown in Fig. 4.

### 3.5. Time-Temperature Superposition Principle

The influence of speed (in a range of 50–100 km/h) on these parameters is rather low. The dissipated energy curve moves to the left with decreasing speed (Fig. 7).

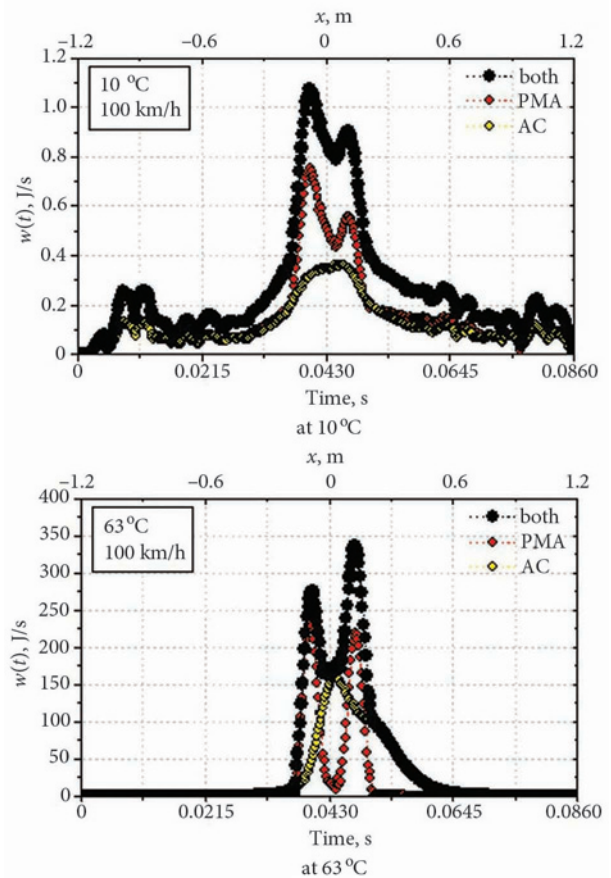


Fig. 6. Evolution of the pavement structure-induced energy dissipation at 100 km/h for a 40 t truck

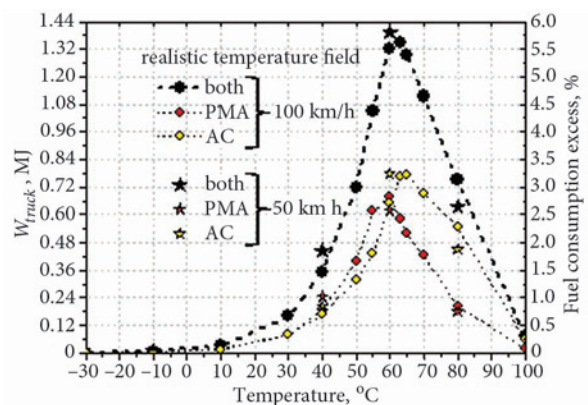


Fig. 7. Evolution of dissipated energy and fuel consumption excess with temperature at 100 km/h and 50 km/h for a 40 t truck



To quantify the displacement of the dissipated energy curve, the latter is plotted for two different constant speeds (50 km/h and 100 km/h) on the same figure. The evolution of the shift factors  $a_T$  used for the building of the master curves of the two considered bituminous materials PMA and AC is also represented functions of temperature (Fig. 8). Shift factors  $a_T$  are very close between the two bituminous mixes (PMA and AC). A WLF law considering average coefficients ( $C_1 = 35$  and  $C_2 = 210$ ) is therefore used. Then a three-step method is proposed.

– Step 1 – read the desired dissipated energy value on the left axis and intercept the dissipated energy curve plotted for two vehicle speeds 50 km/h and 100 km/h.

– Step 2 – read the corresponding temperature  $T$  (for each vehicle speed value) on the horizontal axis.

– Step 3 – read the shift factor  $a_T$  corresponding to the temperatures defined during Step 2.

This method has been applied for three values located before (1.33 MJ), on (0.63 MJ) and after (0.44 MJ) the peak of dissipated energy (Fig. 8).

It can be observed that the ratio between the shift factors obtained for two speeds (100 km/h and 50 km/h) during Step 3 of previous method, is equal to the speeds ratio (namely 2) (Eq (9)).

$$\frac{100 \text{ km/h}}{50 \text{ km/h}} = 2 = \frac{a_T(40^\circ\text{C})}{a_T(42^\circ\text{C})} = \frac{a_T(60^\circ\text{C})}{a_T(63^\circ\text{C})} = \frac{a_T(80^\circ\text{C})}{a_T(84^\circ\text{C})} \quad (9)$$

The TTSP can be therefore used to determine the dissipated energy evolution with temperature at any vehicle speed for a fixed pavement structure.

From the curve of fuel consumption excess at 100 km/h, dissipated energy is calculated using the TTSP for three vehicle speeds: 1 km/h, 50 km/h and 130 km/h (Fig. 8). As a confirmation, complementary simulations at 1 km/h using FEM are also represented for three temperatures, i.e., 28 °C, 45 °C and 63 °C.

First, values calculated using the TTSP for the two speeds 1 km/h and 50 km/h are very close to the ones calculated using FE. In addition, it is clear that the lower speed the lower temperature at which the peak of dissipated energy appears. For instance, at 1 km/h, the maximum of energy dissipation occurs at about 45 °C.

4. Summary and conclusions

In this paper the method to evaluate the dissipated energy in a classical French pavement structure due to viscous properties of bituminous constituent materials is developed. The method is divided into three steps that should be followed whatever the materials, the rheological model or the Finite Element software are used.

1. First, a 3D experimental characterization of two typical bituminous materials was carried out. Their linear behaviour, supposed to be isotropic, was completely defined.

2. The DBN model was then calibrated and used, which constitutes the second step of the proposed method. Its ability to simulate the behaviour of each material is shown. This model was implemented in a finite element code allowing for the simulation of a pavement structure composed of the two characterized bituminous materials.

3. In a third step, simulations of a rolling wheel on the pavement structure were performed using the Finite Element software. From these simulations, the dissipated energy for a 40 t truck was estimated. The results were also expressed as an estimated fuel excess consumption. In particular, results show that, for very unfavourable condition, at 63 °C, the dissipated energy may represent up to 5.5% of the total energy consumed to make the truck moving at a speed of 100 km/h. Yet, at 15 °C (reference mean temperature for pavement design in France) and for the same vehicle speed of 100 km/h, the increase in fuel consumption is limited to 0.25%. At low temperature (< 15 °C) and at very high temperature the dissipated energy is very low as bituminous material is considered as purely elastic in a first approximation.

4. The influence of speed (in a range of 1–130 km/h) on the dissipated energy is rather high. It can be noticed that the dissipated energy curve moves to the left with

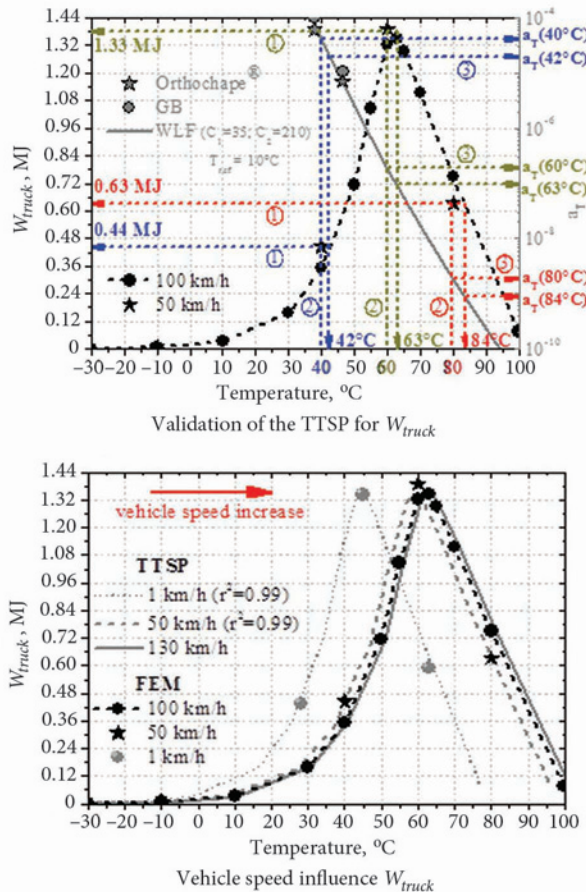


Fig. 8. Validation of the TTSP and analysis of vehicle speed influence for dissipated energy

decreasing speed according to the Time-Temperature Superposition Principle.

This study does not promote rigid pavements compared to flexible pavements. It proposes a scientific method to access fuel consumption excess due to viscous energy dissipation which proves to have a small influence compared to evenness and roughness in flexible and rigid pavements.

In future works, it should be interesting to check the influence of vehicle type (e.g. passenger cars) and different bituminous material and pavement structures. It is also planned to improve calculation by taking into account the evolution of temperature with depth and the influence of dual wheel or tandem axle.

### Acknowledgment

This work has been conducted within the framework of a partnership between the Building and Civil Engineering Department (DGCB) of the University of Lyon/ENTPE (“Ecole Nationale des Travaux Publics de l’Etat”) and the Research and Development Department of the EIFFAGE Travaux Publics Company.

### References

- Baaj, H.; Di Benedetto, H.; Chaverot, P. 2005. Effect of Binder Characteristics on Fatigue of Asphalt Pavement Using an Intrinsic Damage Approach, *Road Materials and Pavement Design* 6(2): 147–174.  
<http://dx.doi.org/10.1080/14680629.2005.9690003>
- Beuving, E.; De Jonghe, T.; Goos, D.; Lindahl, T.; Stawiarski, A. 2004. Fuel Efficiency of Road Pavements, in *The 3<sup>rd</sup> Eurasphalt and Eurobitume Congress*. May 12–14, 2004, Vienna. ISBN 90-802884-4-6.
- Christophe, Th.; Delanne, Y.; Serfass, J. P. 1993. Les Caractéristiques de Surface – Résistance au Roulement, Confort Vibratoire et Caractéristiques de Surface, *Revue Générale des Routes et des Aéroports* 708: 13–7. [in French]
- Chupin, O.; Piau, J.-M.; Chabot, A. 2010. Effect of Bituminous Pavement Structures on the Rolling Resistance, in *the 11<sup>th</sup> International Conference On Asphalt Pavements (ISAP)*. August 1–6, 2010, Nagoya, Aichi, Japan.
- Delaporte, B.; Di Benedetto, H.; Chaverot, P.; Gauthier, G. 2009. Linear Viscoelastic Properties of Bituminous Materials Including New Products Made with Ultrafine Particles, *Road Materials and Pavement Design* 10(1): 7–38.  
<http://dx.doi.org/10.1080/14680629.2009.9690180>
- Di Benedetto, H.; Nguyen, Q. T.; Sauzeat, C. 2011. Nonlinearity, Heating, Fatigue and Thixotropy during Cyclic Loading of Asphalt Mixtures, *Road Materials and Pavement Design* 12(1): 129–158.  
<http://dx.doi.org/10.1080/14680629.2011.9690356>
- Di Benedetto, H.; Sauzéat, C.; Sohm, J. 2009. Stiffness of Bituminous Mixtures Using Ultrasonic Waves Propagation, *Road Materials and Pavement Design* 10(4): 789–814.  
<http://dx.doi.org/10.1080/14680629.2009.9690227>
- Di Benedetto, H.; Neifar, M.; Sauzeat, C.; Olard, F. 2007. Three-Dimensional Thermo-Viscoplastic Behaviour of Bituminous Materials: the DBN Model, *Road Materials and Pavement Design* 8(2): 285–315.  
<http://dx.doi.org/10.1080/14680629.2007.9690076>
- Di Benedetto, H.; De la Roche, C.; Baaj, H.; Pronk, A.; Lundström, R. 2004. Fatigue of Bituminous Mixtures, *Materials and Structures* 37(3): 202–216.  
<http://dx.doi.org/10.1007/BF02481620>
- Du Plessis, H.; Visser, A.; Curtayne, P. 1990. Fuel Consumption of Vehicles as Affected by Road-Surface Characteristics, in *Surface Characteristics of Roadways: International Research and Technologies*. Ed. by Meyer, W. E.; Reichert, J. 480–496.  
<http://dx.doi.org/10.1520/STP23383S>
- Ferry, J. D. 1980. *Viscoelastic Properties of Polymers*. 3<sup>rd</sup> edition. John & Sons. ISBN 9780471048947. 672 p.
- Ihs, A.; Magnusson, G. 2000. *The Significance of Various Road Surface Properties for Traffic and Surroundings*. Project No. 80371. 29 p.
- Laganier, R.; Lucas, J. 1990. The Influence of Pavement Evenness and Macrotecture on Fuel Consumption, *Surface Characteristics of Roadways: International Research and Technologies* 454–459.
- Lundström, R.; Di Benedetto, H.; Isacsson, U. 2004. Influence of Asphalt Mixture Stiffness on Fatigue Failure, *Journal of Materials in Civil Engineering* 16(6): 516–525.  
[http://dx.doi.org/10.1061/\(ASCE\)0899-1561\(2004\)16:6\(516\)](http://dx.doi.org/10.1061/(ASCE)0899-1561(2004)16:6(516))
- Mangiafico, S.; Di Benedetto, H.; Sauzéat, C.; Olard, F.; Pouget, S.; Planque, L. 2013. Influence of Reclaimed Asphalt Pavement Content on Complex Modulus of Asphalt Binder Blends and Corresponding Mixes: Experimental Results and Modelling, *Road Materials and Pavement Design* 14 (Suppl. 1, Special Issue: EATA 2013): 132–148.  
<http://dx.doi.org/10.1080/14680629.2013.774751>
- Neifar, M.; Di Benedetto, H. 2001. Thermo-Viscoplastic Law for Bituminous Mixes, *Road Materials and Pavement Design* 2(1): 71–95. <http://dx.doi.org/10.1080/14680629.2001.9689894>
- Nguyen, Q. T.; Di Benedetto, H.; Sauzéat, C. 2012. Determination of Thermal Properties of Asphalt Mixtures as Another Output from Cyclic Tension–Compression Test, *Road Materials and Pavement Design* 13(1): 85–103.  
<http://dx.doi.org/10.1080/14680629.2011.644082>
- Nguyen, H. M.; Pouget, S.; Di Benedetto, H.; Sauzéat, C. 2009. Generalization of the Time-Temperature Superposition Principle for Bituminous Mixtures: Experimentation and Modeling, *European Journal of Environmental and Civil Engineering* 13(9): 1095–1107.  
<http://dx.doi.org/10.1080/19648189.2009.9693176>
- Olard, F.; Di Benedetto, H. 2005. The DBN Model: a Thermo-Visco-Elasto-Plastic Approach for Pavement Behavior Modeling, *Journal of the Association of Asphalt Paving Technologists* 74: 791–828.
- Pouget, S.; Loup, L. 2013. Thermo-Mechanical Behaviour of Mixtures Containing Bio-Binders, *Road Material and Pavement Design* 14(Suppl. 1, Special Issue: EATA 2013): 212–226.  
<http://dx.doi.org/10.1080/14680629.2013.774758>
- Pouget, S.; Sauzéat, C.; Di Benedetto, H.; Olard, F. 2012a. Modeling of Viscous Bituminous Wearing Course Materials on Orthotropic Steel Deck, *Materials and Structures* 45(7): 1115–1125. <http://dx.doi.org/10.1617/s11527-011-9820-z>

- Pouget, S.; Sauzéat, C.; Di Benedetto, H.; Olard, F. 2012b. Viscous Energy Dissipation in Asphalt Pavement Structures and Implication on Vehicle Fuel Consumption, *Journal of Materials in Civil Engineering* 24(5): 568–576. [http://dx.doi.org/10.1061/\(ASCE\)MT.1943-5533.0000414](http://dx.doi.org/10.1061/(ASCE)MT.1943-5533.0000414)
- Pouget, S.; Sauzéat, C.; Di Benedetto, H.; Olard, F. 2012c. Effect of Vehicle Speed on Millau Viaduct Response, *ASTM International Journal of Testing and Evaluation* 40(7): 1–7. <http://dx.doi.org/10.1520/JTE20120127>
- Pouget, S.; Sauzéat, C.; Di Benedetto, H.; Olard, F. 2010a. From the Behavior of Constituent Materials to the Calculation and Design of Orthotropic Bridge Structures, *Road Materials and Pavement Design* 11: 111–144. <http://dx.doi.org/10.1080/14680629.2010.9690329>
- Pouget, S.; Sauzéat, C.; Di Benedetto, H.; Olard, F. 2010b. Numerical Simulation of the Five-Point Bending Test Designed to Study Bituminous Wearing Courses on Orthotropic Steel Bridge, *Materials and Structures* 43(3): 319–330. <http://dx.doi.org/10.1617/s11527-009-9491-1>
- Raab, C.; Abd El Halim, O.; Partl, M. N. 2013. Utilisation of Artificial Neural Network for the Analysis of Interlayer Shear Properties, *The Baltic Journal of Road and Bridge Engineering* 8(2): 107–116. <http://dx.doi.org/10.3846/bjrbe.2013.14>
- Sandberg, U. 1990. Road Macro- and Megatexture Influence on Fuel Consumption, *Surface Characteristics of Roadways: International Research and Technologies* 460–479. <http://dx.doi.org/10.1520/STP23382S>
- Tiouajni, S.; Di Benedetto, H.; Sauzéat, C.; Pouget, S. 2011. Approximation of Linear Viscoelastic Model by Generalized Kelvin Voigt or Generalized Maxwell Models: Application to Bituminous Materials in the 3 Dimensional Case, *Road Materials and Pavement Design* 12(4): 897–930. <http://dx.doi.org/10.1080/14680629.2011.9713899>
- Williams, A. 1981. Aspects of Tyre/Road Properties Relatable to Driver Comfort and Safety, *Highways and Public Works* 1854: 10–13.
- Zaniewski, J. 1983. Fuel Consumption Related to Roadway Characteristics, *Transportation Research Record* 901: 18–29.
- Zaniewski, J. P.; Moser, B.; De Morais, P. J.; Kaeschagen, R. L. 1979. Fuel Consumption Related to Vehicle Type and Road Conditions, *Transportation Research Record* 702: 328–334.

Received 16 January 2012; accepted 23 February 2012